April 19th 2009

The Casimir Effect

Version 3

A Comprehensive Exercise by

Kyle Kingsbury

Abstract

The Casimir Effect is a small force on conducting surfaces which arises from quantum electrodynamics. Quantizing the electromagnetic field yields a small ground-state energy for each frequency. Summing over all frequencies implies the field has an infinite vacuum energy. Between conducting surfaces, this energy may be dependent on geometry, which gives rise to forces on the boundaries. This comprehensive exercise explores the electromagnetic ground state energy and the consequent force between two conducting plates. Some extensions and generalizations of the Casimir force to other geometries and temperatures are discussed. Finally, it offers a brief overview of experimental attempts to confirm the effect.

Contents

1 Introduction

Weird things happen in nature. Physicists, concerned with modeling and predicting the fundamental dynamics that underlie the observable universe, frequently find themselves discussing things which—to our everyday physical intuition—might seem completely impossible, yet the physics works. Moreover, the physical predictions are backed up by rigorous experiments! Take, for example, special relativity's upending of any notion of a universal coordinate time; or the mind-boggling Stern-Gerlach experiments which demonstrate that probabilities are fundamentally complex[1] states [1, 2]. So perhaps, it is not so unreasonable to predict an infinite energy which is present even in empty space, entwined with the quantum fields which propagate light, electricity, and magnetism, and giving rise to real forces on macroscopic objects. This mysterious energy produces, in the appropriate configurations, the *Casimir effect*.

Electricity and magnetism are governed, in classical mechanics, by Maxwell's equations: relations which describe the interplay of the magnetic and electric fields. These equations describe the fields which allow magnets to stick to refrigerators and hair to float towards balloons after rubbing. Maxwell's equations may also give rise, in empty space, to certain oscillating propagations of electric and magnetic fields called "plane waves" [3]. As it turns out, these waves are related to a well-known mathematical construct known as a *simple harmonic oscillator*. This suggests that the electromagnetic field itself may be modeled, in some form, as a harmonic oscillator as well.

In classical mechanics, simple harmonic oscillators (and hence light waves) may have any energy, but in the quantum formalism, simple harmonic oscillators have specific energies of the form

$$E(n) = (1/2 + n)\hbar\omega \tag{1.1}$$

where $\hbar = 1.0546 \times 10^{-34}$ J $\cdot$ s is a fundamental constant of energy $\times$ time, and ω is the frequency of the oscillator. Unlike the classical harmonic oscillator, the quantum harmonic oscillator can never possess zero energy. In fact, its least energetic, or "ground" state has energy $1/2\hbar\omega$. As it turns out, this ground energy implies that even in an electromagnetic system which has no photons, some energy remains.

In quantum field theory, we represent the electromagnetic field as an operator which is analogous to the sum of an infinite number of harmonic oscillators (one for each frequency). The ground state energy is therefore a sum over infinite frequencies—an infinite quantity itself. This field structure

[1] In the mathematical sense: $a + bi$.

gives rise to an infinite energy in empty space.

Under ordinary circumstances this energy is unnoticeable. It exists wherever the electromagnetic field does. Yet, as only differences in energy give rise to forces, we rarely feel the field energy's effects. However, by introducing certain types of boundary conditions on the field, we can change the allowed frequencies for the system—resulting in a lower energy density in one part of space. These differentials give rise to a small but experimentally observable force on the boundaries, known as the Casimir effect.

We'll start by proving the quantization conditions outlined above in Section 2, move on to explore the energy between two parallel conducting plates in Section 3, and compare two schemes for renormalizing the infinities associated with quantum electrodynamics. In Sections 4, 5, and 6, we will discuss various applications, geometries, and extensions of the Casimir effect. Finally, Section 7 highlights some of the key experimental literature in the field: evidence for the surprising reality of this counterintuitive phenomenon.

2 Quantizing the Electromagnetic Field

We begin with Maxwell's equations [3].

$$\nabla \cdot \mathbf{E} = \frac{\rho}{\epsilon_0} \tag{2.1}$$

$$\nabla \times \mathbf{E} = -\frac{\partial \mathbf{B}}{\partial t} \tag{2.2}$$

$$\nabla \cdot \mathbf{B} = 0 \tag{2.3}$$

$$\nabla \times \mathbf{B} = \mu_0 \mathbf{J} + \mu_0 \epsilon_0 \frac{\partial \mathbf{E}}{\partial t} \tag{2.4}$$

Equation (2.1) implies the existence of the scalar potential ϕ, and Lorentz invariance promotes this potential to a full vector potential $\mathbf{A}$ [4]. Using these, we can rewrite (2.3) and (2.4) as:

$$-\nabla^2 \phi - \frac{1}{c}\frac{\partial}{\partial t}\nabla \cdot \mathbf{A} = 4\pi\rho \tag{2.5}$$

$$\nabla(\nabla \cdot \mathbf{A}) - \nabla^2 \mathbf{A} = \frac{4\pi}{c}\mathbf{J} + \frac{1}{c}\frac{\partial}{\partial t}\left(-\nabla\phi - \frac{1}{c}\frac{\partial \mathbf{A}}{\partial t}\right). \tag{2.6}$$

When no charges or currents are present, both ρ and $\mathbf{J}$ are zero. The Hamiltonian for the

electromagnetic field is then[2]

$$H_{EM} = \frac{1}{8\pi} \int (\mathbf{E}^2 + \mathbf{B}^2)\, d^3r. \tag{2.7}$$

In the absence of charges or currents, the definition of the vector potential allows us to write

$$H_{EM} = \frac{1}{8\pi} \int \left[\left(-\frac{1}{c} \frac{\partial \mathbf{A}}{\partial t} \right)^2 + (\nabla \times \mathbf{A})^2 \right] d^3r. \tag{2.8}$$

We take as granted the Hermitian operator form of the vector potential [2]:

$$\hat{\mathbf{A}} = \sum_{\mathbf{k},\lambda} c \sqrt{\frac{w\pi\hbar}{\omega}} \left(\hat{a}_{\mathbf{k},\lambda} \epsilon(\mathbf{k},\lambda) \frac{e^{i(\mathbf{k}\cdot\mathbf{r} - \omega t)}}{\sqrt{V}} + \hat{a}^\dagger_{\mathbf{k},\lambda} \epsilon(\mathbf{k},\lambda) \frac{e^{-i(\mathbf{k}\cdot\mathbf{r} - \omega t)}}{\sqrt{V}} \right). \tag{2.9}$$

Here, $\mathbf{k}$ is a wavevector in the direction of propagation whose magnitude determines the frequency of the wave. λ is a polarization term, ω is the angular frequency, ϵ is a function which ensures terms have the correct sign and magnitude, and $\hat{a}^\dagger$ and $\hat{a}$ are the raising and lowering operators satisfying

$$\left[\hat{a}_{\mathbf{k},\lambda}, \hat{a}^\dagger_{\mathbf{k}',\lambda'} \right] = \delta_{\mathbf{k},\mathbf{k}'} \delta_{\lambda,\lambda'}. \tag{2.10}$$

These operators act on the state of the electromagnetic field at the frequency and spin corresponding to their $\mathbf{k}$ and λ. When $\hat{a}^\dagger_{\mathbf{k},\lambda}$ acts on a state, it increases the energy of by $\hbar\omega$. $\hat{a}_{\mathbf{k},\lambda}$ inverts the process, lowering the energy of the mode by $\hbar\omega$. Therefore, we conceptualize $\hat{a}^\dagger$ as a *creation operator* which adds a single photon to the field, and $\hat{a}$ as an *annihilation operator* which removes a photon. The creation and annihilation approach makes it easy to analyze the Hamiltonian; by substituting (2.9) for the vector potential in (2.8), we find

$$\begin{aligned} \hat{H} &= \frac{1}{2} \sum_{\mathbf{k},\lambda} \hbar\omega \left(\hat{a}_{\mathbf{k},\lambda} \hat{a}^\dagger_{\mathbf{k},\lambda} + \hat{a}^\dagger_{\mathbf{k},\lambda} \hat{a}_{\mathbf{k},\lambda} \right) \\ &= \sum_{\mathbf{k},\lambda} \hbar\omega \left(\hat{a}^\dagger_{\mathbf{k},\lambda} \hat{a}_{\mathbf{k},\lambda} + \frac{1}{2} \right), \end{aligned} \tag{2.11}$$

thanks to the commutation relations for $\hat{a}^\dagger$ and $\hat{a}$.

The ground state for this Hamiltonian (written $|0\rangle$) is defined by

$$\hat{a}_{\mathbf{k},\lambda} |0\rangle = 0. \tag{2.12}$$

[2]Here we are assuming the use of the Coulomb gauge $\nabla \cdot \mathbf{A} = 0$. Gauge choice does not affect the derived ground state energy [5].

in other words, the state from which no more photons can be annihilated. This is an empty electromagnetic field: every mode has no photons present, and is in its lowest possible energy state.

Because the raising and lowering operators commute whenever $\mathbf{k}$ or λ are different, we can decompose $|0\rangle$ into the product of each independent oscillator for a given $\mathbf{k}$ and λ:

$$|0\rangle = |0_{\mathbf{k}_1,\lambda_1}\rangle \otimes |0_{\mathbf{k}_2,\lambda_2}\rangle \otimes |0_{\mathbf{k}_3,\lambda_3}\rangle \otimes \cdots \tag{2.13}$$

where the tensor product $|\text{spin up}\rangle \otimes |x = 0\rangle$ denotes the state in which the system is both spin up and at $x = 0$.

Classically, we expect that an electromagnetic field with no photons would have zero energy. However, when we take the expectation value of the Hamiltonian (2.8) acting on $|0\rangle$, we find

$$\langle 0|\, \hat{H}\, |0\rangle = \langle 0| \sum_{\mathbf{k},\lambda} \hbar\omega \left(\hat{a}^\dagger_{\mathbf{k},\lambda} \hat{a}_{\mathbf{k},\lambda} + \frac{1}{2} \right) |0\rangle \tag{2.14}$$

$$\langle E \rangle = \frac{1}{2} \sum_{\mathbf{k},\lambda} \hbar\omega. \tag{2.15}$$

Hence the energy of the electromagnetic field in the ground state is the sum of many uncoupled harmonic oscillators, each with energy $1/2\hbar\omega$. Why is the energy non-zero? One way to rationalize this result is to recognize that the commutation relation of $\langle \mathbf{E} \rangle$ and $\langle \mathbf{B} \rangle$ is [6]

$$\left[\hat{\mathbf{E}}_j(\mathbf{x}), \hat{\mathbf{B}}_k(\mathbf{y}) \right] = -\imath\hbar\mu_0 c^2 \epsilon_{jkl} \delta_{,l}(\mathbf{x} - \mathbf{y}), \tag{2.16}$$

which implies that the electric and magnetic fields do not (in general) commute. Therefore, over time, they should exhibit small quantum fluctuations greater than zero. Their fluctuations cannot vanish unless $[\mathbf{E}, \mathbf{B}]$ is zero, so we should expect some energy to be present in the system.

What is more surprising is that this zero-point energy is infinite, being a sum over all possible frequencies. Equation (2.15) states that empty space, thanks to the dynamics of the electromagnetic field operators, has an infinite, intrinsic energy—even when no photons are present. Under ordinary conditions this infinity is not physically measurable, as it is present at each point in space. As we will see, however, imposing boundary conditions on the electromagnetic field can generate *differences* in the zero-point energy, which will lead to surprising results.

3 The Force Between Two Plates

To illustrate the most basic example of the Casimir effect, we consider the same system that Casimir evinced in his second 1948 paper: the vacuum energy of two parallel conducting plates brought very close together [7]. Instead of taking a classical electromagnetic approach and including retardation effects, he derived their interaction energy from a quantum-mechanical perspective. This section presents a slightly modified version of Casimir's original derivation, and compare it with a more modern zeta-functional renormalization program.

3.1 Casimir's Derivation

Consider a conducting box of volume L^3, with an $L \times L$ plate contained within, parallel to the x and y axes of the box. We let the distance between the plate and the wall of the box be a, and vary a to find the change in vacuum energy.

The conducting walls of the box impose Dirichlet boundary conditions on the possible electromagnetic modes of the cavity: the tangential component of the electromagnetic field must vanish there. Solving the wave equation with these conditions[3] reveals that the boundaries quantize the x, y, and z components of the wavevectors $\mathbf{k}$, such that they take on the discrete values

$$k_x = \frac{\pi}{L} n_x, \quad k_y = \frac{\pi}{L} n_y, \quad k_z = \frac{\pi}{a} n_z. \tag{3.1}$$

where

$$k^2 = k_x^2 + k_y^2 + k_z^2. \tag{3.2}$$

In a vacuum, angular frequency ω is related to the wave number k by the speed of light c:

$$\omega = ck. \tag{3.3}$$

This allows us to express the zero-point energy of the field (2.15) as a sum over quantized modes, identified by k_x, k_y, and k_z:

$$\langle E \rangle = \hbar c \sum \frac{1}{2} \sqrt{k_x^2 + k_y^2 + k_z^2}. \tag{3.4}$$

Polarization (the λ terms in section 2) allows for two waves corresponding to each wave number—

[3] A well-known Sturm-Liouville problem.

except when one k_i is 0.[4] Therefore, we multiply all $k > 0$ terms by 2, and expand the summation in x, y, and z:

$$\langle E \rangle = \hbar c \sum_{n_x=0}^{\infty} \sum_{n_y=0}^{\infty} \left[\frac{1}{2} \sqrt{\left(\frac{n_x \pi}{L}\right)^2 + \left(\frac{n_y \pi}{L}\right)^2} + \sum_{n_z=1}^{\infty} \sqrt{\left(\frac{n_x \pi}{L}\right)^2 + \left(\frac{n_y \pi}{L}\right)^2 + \left(\frac{n_z \pi}{a}\right)^2} \right] \tag{3.5}$$

Since x and y are presumed to be very large compared to a, we treat them as continuous variables and convert their sums to integrals, writing

$$\langle E \rangle = \hbar c \int_0^{\infty} \int_0^{\infty} \frac{1}{2} \sqrt{\left(\frac{n_x \pi}{L}\right)^2 + \left(\frac{n_y \pi}{L}\right)^2} + \sum_{n_z=1}^{\infty} \sqrt{\left(\frac{n_x \pi}{L}\right)^2 + \left(\frac{n_y \pi}{L}\right)^2 + \left(\frac{n_z \pi}{a}\right)^2} \, dn_x \, dn_y \tag{3.6}$$

We now consider the three dimensional parameter space n_x, n_y, n_z. Observing that the x and y terms are added in quadrature, we make a change to polar coordinates $x^2 = k_x^2 + k_y^2$. The resulting substitution from $n_{x,y} \to k_{x,y}$ yields an additional factor of L^2/π^2, and integrating over the radial angle for the first quadrant (all quantities are positive) gives $\pi/2$. We let $n = n_z$ for brevity, and obtain

$$\langle E \rangle = \hbar c \frac{L^2}{\pi^2} \frac{\pi}{2} \int_0^{\infty} \sum_{n=(0)1}^{\infty} \sqrt{\left(\frac{n\pi}{a}\right)^2 + x^2} \; x \, dx \tag{3.7}$$

In the above sum, (0)1 indicates that the term with $n = 0$ is to be multiplied by 1/2.

$\langle E \rangle$ is clearly infinite. The series diverges exponentially, and the integral diverges quicker still. This result makes some degree of physical sense. Quantizing the electromagnetic field at each point in continuous space must yield an infinite energy. However, for purposes of mechanics, we are free to set the zero of a potential energy wherever we like—even at infinity. To that end, we consider the difference between the vacuum point energy at two configurations: one where a is on the order of $L/2$, and another in which it is much smaller.

$$\delta E = \hbar c \frac{L^2}{\pi^2} \frac{\pi}{2} \left[\sum_{n=(0)1} \int_0^{\infty} \sqrt{k_z^2 + x^2} \; x \, dx - \int_0^{\infty} \int_0^{\infty} \sqrt{k_z^2 + x^2} \; x \, dx \; \left(\frac{a}{\pi} \, dk_z\right) \right] \tag{3.8}$$

The first term corresponds to small (discrete) a. The second term treats a as large enough to be continuous, and converts the sum to an integral accordingly. In effect we are subtracting the quantized energy within the cavity from the intrinsic energy in free space, as shown in Figure 3.1.

[4] This apparent special case arises from the "folding over" of the sum over both positive and negative $\mathbf{k}$ (from $-\infty$ to ∞) into a sum from 0 to ∞—which simplifies evaluation later.

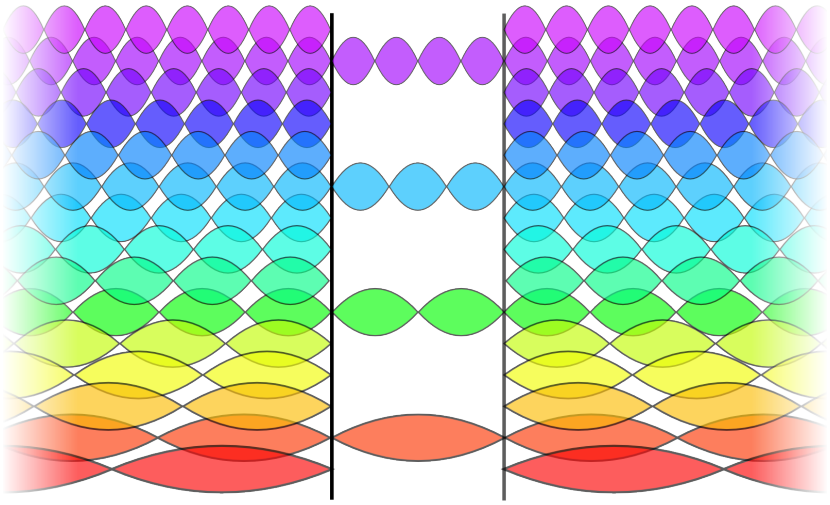

Figure 1: Outside the cavity formed by the plates, all vacuum frequencies are allowed. Within the cavity, however, the vacuum modes take on discrete frequencies. Changing the width of the cavity changes the density of modes relative to free space, which yields an energy difference.

To simplify the integrand, we introduce a dummy variable

$$u \equiv \left(\frac{ax}{\pi}\right)^2 \tag{3.9}$$

and perform a change of variables:

$$\begin{aligned} \delta E &= \hbar c \frac{L^2}{\pi^2}\frac{\pi}{2}\left[\sum_{n=(0)1}^{\infty}\int_0^\infty \frac{\pi}{a}\sqrt{n^2+u}\,\frac{\pi^2}{2a^2}\,du - \int_0^\infty\int_0^\infty \frac{\pi}{a}\sqrt{n^2+u}\,\frac{\pi^2}{2a^2}\,du\,dn\right] \\ &= L^2\hbar c\frac{\pi^2}{4a^3}\left[\sum_{n=(0)1}^{\infty}\int_0^\infty \sqrt{n^2+u}\,du - \int_0^\infty\int_0^\infty \sqrt{n^2+u}\,du\,dn\right]. \end{aligned} \tag{3.10}$$

Unfortunately, even this energy difference is divergent! Luckily, we can avoid this difficulty by considering the fact that each conductor has a plasma frequency

$$\omega_p^2 = \frac{Nq^2}{m_e\epsilon_0}, \tag{3.11}$$

which is the minimum oscillation frequency the electrons in the conductor can support [8]. Below the

plasma frequency, the conductor acts as a reactive medium[5] and reflects electromagnetic waves—giving rise to the boundary conditions discussed above. Above the plasma frequency, however, the electrons are capable of oscillating in resonance with the waves. This means that the conductor is effectively transparent to photons above a certain frequency, and the boundary conditions no longer hold. Because of this, we multiply the contributions to the total energy of each mode k by a regulator function $f(k/k_m)$ which is unity for $k \ll k_m$, approaches 0 at infinity, and is 1/2 at $k = k_m$. The exact value of k_m and the shape of f may be phenomenologically obtained, but will not be especially important in the final approximation. We obtain

$$\delta E = L^2 \hbar c \frac{\pi^2}{4a^3} \left[\sum_{n=(0)1}^{\infty} \int_0^{\infty} \sqrt{n^2 + u}\, f(\pi\sqrt{n^2+u}/ak_m)\, du \right. \\ \left. - \int_0^{\infty} \int_0^{\infty} \sqrt{n^2 + u}\, f(\pi\sqrt{n^2+u}/ak_m)\, du\, dn \right]. \quad (3.12)$$

In quantum mechanics, many important problems involve divergent sums or integrals, yet we have good reason to believe the observables they describe are finite. For example, if the energy difference between two plates were truly infinite, we would expect extreme results. Two mirrors placed close together would snap closed and never come apart! Therefore, we use two techniques to work around the infinities and make useful predictions: regularization, and renormalization.

Introducing $f(k/k_m)$ comprises our regularization step. We transformed the infinite expression into a finite one by introducing a special function. Here, we made a reasonable physical argument for the introduction of a cutoff function, but in other cases, no physical argument is available. One may then choose to say that the regularization is a consequence of some unspecified physics [5]. Alternatively, one could argue that the mathematical expression of the quantity being measured does not truly correspond to the dynamics; the renormalization is a way to bring the mathematics back into correspondence with reality.

In either case, the key to an effective renormalization program is to show that the answer is independent of the regularization parameters [5]. For example, we could take the limit of the cutoff frequency to infinity, after obtaining a finite sum. In some configurations of the Casimir effect, the Riemann Zeta function is used, through analytic continuation, to bring the infinities under control. In Casimir's plate derivation, however, renormalization is somewhat simpler.

[5] *Reactive*, in this case, means a medium which only propagates exponentially decaying waves.

Returning to δE, we introduce $w \equiv u + n^2$, obtaining[6]

$$\delta E = L^2 \hbar c \frac{\pi^2}{4a^3} \left[\sum_{n=(0)1}^{\infty} \int_{n^2}^{\infty} \sqrt{w}\, f(\pi\sqrt{w}/ak_m)\, dw - \int_0^{\infty} \int_{n^2}^{\infty} \sqrt{w}\, f(\pi\sqrt{w}/ak_m)\, dw\, dn \right] \tag{3.13}$$

This type of expression—the difference between a sum and an integral—was considered by both Euler and Maclaurin around 1735 [9]. Both found, independently, that for a smooth function $F(x)$:

$$\int_0^N f(x)\, dx - \sum_{n=(0)1}^{(N)} f(n) = \sum_{k=2}^{p} \frac{B_k}{k!} \left(f^{(k-1)}(N) - f^{(k-1)}(0) \right) + R \tag{3.14}$$

where R is a decreasing error term. B_k are the Bernoulli numbers (-1/2, 1/6, 0, -1/30, 0, 1/42, ...). Identifying $F(n)$ with the inner integral in both terms and applying the fundamental theorem of calculus, we recover $F'(n)$ and the subsequent derivatives which will appear in the Euler-Maclaurin series.

$$F(n) = \int_{n^2}^{\infty} \sqrt{w}\, f(\pi\sqrt{w}/ak_m)\, dw \tag{3.15}$$

$$F'(n) = -2n^2 f(n\pi/ak_m) \tag{3.16}$$

$$F''(n) = -4nf(n\pi/ak_m) - 2n^2 f'(n\pi/ak_m) \left(\frac{\pi}{ak_m} \right) \tag{3.17}$$

$$F'''(n) = -4f(n\pi/ak_m) - 8nf'(n\pi/ak_m) \left(\frac{\pi}{ak_m} \right) - 2n^2 f''(n\pi/ak_m) \left(\frac{\pi}{ak_m} \right)^2 \tag{3.18}$$

Considering the characteristics of $f(k/k_m)$ at 0 and ∞ allows us to fill in the first few terms of (3.14).

$$\delta E = L^2 \hbar c \frac{\pi^2}{4a^3} \left[\frac{1}{12}(0 - 0) - \frac{1}{720}(0 - (-4)) + \ldots \right] \tag{3.19}$$

Notice that the Euler-Maclaurin summation formula only evaluates $F(n)$ at zero and infinity. This is the final step in our renormalization of the δE divergence. The cutoff frequency can vary from zero to infinity, and—so long as the distance between the plates does not bring the energy scale close to k_m—we may say that the final energy is finite for all systems, regardless of the cutoff behavior. When the energy scale of the system *does* approach the cutoff frequency, the nature of the cutoff function becomes more important and the model may require corrections [5].

Inspection of the derivatives of F reveals that all subsequent terms will involve powers of $\frac{\pi}{ak_m}$.

[6] In Casimir's 1948 paper, the argument to f is taken as w, not $\sqrt{w}$. I have corrected this typo and its consequences in this derivation. The change does not appreciably affect the results, except for higher-order terms in the approximation which we take to be zero.

When this ratio is small—that is, when the cutoff frequency of the conductor is sufficiently large compared to the distance between the plates—the remaining terms in the series are negligible and we may approximate

$$\delta E \approx -L^2 \hbar c \frac{\pi^2}{720} \frac{1}{a^3}. \tag{3.20}$$

If we vary a slowly and adiabatically, we find that the pressure[7] is related to the energy by [10]

$$\begin{aligned} P &= -\frac{\partial E}{\partial V} \\ &= -\hbar c \frac{\pi^2}{240} \frac{1}{a^4}, \end{aligned} \tag{3.21}$$

which is the expression often referred to as "the Casimir force". What does this force mean? In his original derivation, Casimir observed that since the sign is negative with respect to a, the energy of the electromagnetic vacuum gives rise to an *attractive* force between the plates, which scales as a^{-4}. Moreover, the attraction does not depend on the conductor's materials, so long as the distance between the plates a is significantly larger than the penetration depth of the waves in the cavity, as determined by k_m. At very close distances, the approximation breaks down as the electromagnetic waves start to leak through the cavity walls.

Moreover, the expression includes a factor of $\hbar$. As $\hbar$ goes to zero[8], the Casimir effect fades. The attraction between plates is a fundamentally quantum result, which arises from the quantization conditions imposed by the harmonic solutions to the electromagnetic field Hamiltonian.

3.2 A Modern Derivation

We reformulate slightly the vacuum energy between the two plates, considering an integral over the parallel waves k_x and k_y and a sum over the perpendicular waves $k_z = n\pi/a$:

$$\langle E(a) \rangle = \frac{\hbar}{2} \int_{-\infty}^{\infty} \int_{-\infty}^{\infty} \frac{1}{(2\pi)^2} \sum_{n=-\infty}^{\infty} \omega L^2 \, dk_x \, dk_y. \tag{3.22}$$

Here, the sum over 2 possible polarization states for all $k \neq 0$ has been accounted for by extending the sum to $-\infty$. We will not be using the Euler-Maclaurin formula, so this form is clearer.

While the renormalization program followed by Casimir in his parallel-plates derivation [7] was

[7] Of our virtual photon gas.

[8] A common way of evaluating the classical behavior of an expression is to consider the limit as $\hbar \to 0$, as in most classical situations $\hbar$ is negligible compared to the energy/time scale of the system.

rooted in sound physical intuition, many modern derivations of the Casimir effect make use of a more advanced mathematical transformation known as *zeta function regularization* [11]. Instead of introducing a cutoff frequency, we force the sum to be convergent by dividing by (potentially complex) powers s of ω. After taking the integral, we will renormalize by taking the limit as $s \to 0$, effectively taking the corrective term to unity. The regularized expression is

$$\langle E(a,s)\rangle = \frac{\hbar}{2}\int_{-\infty}^{\infty}\int_{-\infty}^{\infty}\frac{1}{(2\pi)^2}\sum_{n=-\infty}^{\infty}\omega\cdot\omega^{-2s}L^2\,dk_x\,dk_y. \tag{3.23}$$

We make the same switch to polar coordinates (x,ϕ) in the (x,y) plane, and substitute $y \equiv (ax/n\pi)$:

$$\langle E(a,s)\rangle = \frac{\hbar c}{2\pi}\int_0^{\infty} y(y^2+1)^{1/2-s}\sum_{n=1}^{\infty}\left(\frac{n\pi}{a}\right)^{3-2s}L^2\,dy. \tag{3.24}$$

This expression becomes divergent as $s \to 0$, but it does converge for $s = 3/2$ and larger. Our plan is to evaluate each expression in its domain of convergence, and then to analytically continue to $s = 0$. We treat the integral first, as it is easier:

$$\int_0^{\infty} y(y^2+1)^{1/2-s}\,dy. \tag{3.25}$$

Substitute $u \equiv y^2$, and find

$$\frac{1}{2}\int_0^{\infty}(u+1)^{1/2-s}\,du. \tag{3.26}$$

Introducing $w \equiv u^2$, the integration is trivial.[9] We assume that s is greater than $3/2$, ensuring convergence. The result is then

$$\begin{aligned}&\frac{1}{2}\left(\frac{1}{3/2-s}\right)w^{3/2-s}\Big|_1^{\infty}\\ =\;& -\frac{1}{2}\left(\frac{1}{3/2-s}\right),\end{aligned} \tag{3.27}$$

which may be analytically continued to $-1/3$ at $s = 0$ [12]. Returning to (3.24), factoring out some constants, and taking their limits as $s \to 0$, we obtain:

$$\langle E(a,s)\rangle = -L^2\hbar c\frac{\pi^2}{2\times 3}\frac{1}{a^3}\sum_{n=1}^{\infty}\frac{1}{n^{2s-3}}. \tag{3.28}$$

Evaluating the sum is more difficult. However, we may make the substitution $t \equiv 2s - 3$, to

[9] Provided one is not concerned with domains of convergence.

give

$$\langle E(a,t)\rangle = -L^2\hbar c\frac{\pi^2}{2\times 3}\frac{1}{a^3}\sum_{n=1}^{\infty}\frac{1}{n^t}. \tag{3.29}$$

This last sum is not convergent, but it does have a unique analytic extension. In fact, this particular sum is an extremely well-studied mathematical entity known as the *Riemann zeta function*, denoted $\zeta(t)$ [13]. We are interested in $\zeta(-3)$, which corresponds to $s \to 0$. Unfortunately, this definition of the zeta function is divergent in the complex plane for negative real s, but by evaluating the sum of negative and positive terms, it is possible to extend $\zeta(t)$ from $\mathrm{Re}(s) > 0$ to the whole complex plane. This analytic continuation has been well-studied and its values at certain critical points are well known. In this case, a very simple result is available:

$$\zeta(-3) = 1/120. \tag{3.30}$$

The final energy is therefore

$$\langle E\rangle = -L^2\hbar c\frac{\pi^2}{720}\frac{1}{a^3}, \tag{3.31}$$

which matches Casimir's derivation (3.20). Note, however, that we have *not* subtracted the plate energies in the near and far configurations, as we did in section 3.1. This suggests an important physical intuition for zeta renormalization: using the analytic continuation from $s = 3$ to $s = 0$ in some sense corresponds to subtracting the electromagnetic field's inherent contribution to the ground state energy $\langle E\rangle$ [12, 11]. In Casimir's derivation we removed the infinite contribution of the field by taking the difference of two configurations, in effect subtracting whatever (infinite) energy the field possesses in free space. Here the subtraction may not be as intuitive, but its analytic simplicity makes it a powerful tool for analyzing vacuum energy problems. In fact, the zeta function has a close relationship to the commutators of differential operators, suggesting that the values of s we choose for renormalization correspond to spatial properties of the field under consideration [14].

Zeta function analysis is not optimal for computational methods, as the p-series is very slow to converge [11]. However, it allows us to take advantage of superior analytic techniques which do not require the dependence on an awkward regulator function, and has been successfully applied to a wide domain of problems in quantum electrodynamics [15].

3.3 Other Regularization Techniques

There are some configurations for which the zeta-functional analysis shown above fails. There may still be infinities present in the sum which may not be removed by introducing a factor ω^{-s}. In still others, the renormalization procedure may be unclear. Luckily, there are other techniques for dealing with the infinities in vacuum-energy problems such as the Casimir effect.

One of the most useful and generalizable of these techniques makes use of the photonic Green's function, which describes the susceptibility of the electromagnetic field in a statistical way [16]. Green's functions may then be regularized through dimensional or cutoff techniques [5].

Another technique involves identifying the zeta function as an integral over a function known as the heat kernel, which is a fundamental solution to the heat equation given a certain initial point source of heat. Linear combinations of heat kernels are used to construct general solutions, and by some clever mathematical relations, the eigenvalues of the heat kernel can be related to the coefficients of summation over w in the Casimir energy [11].

4 Atomic Geometry

This section investigates the line of inquiry which led to the two-plates derivation discussed previously, starting with Verwey and Overbeek's experimental disparity in colloidal forces and discussing Casimir and Polder's retardation model for statically polarizable atoms.[10]

4.1 Historical Context

In the 1940s, Verwey and Overbeek were conducting research into colloidal solutions [17]. They developed a theory of the cohesion of colloids (liquid solutions containing a suspension of particles) in which the constituent particles were held together by London-van der Waals forces. However, their predictions for colloids composed of larger particles were experimentally disconfirmed: the attractive force fell faster than the R^{-7} predicted by their model. Overbeek suggested that their model's predictions could become inaccurate as the distance between particles increased. For distances larger than atomic transition wavelengths, the finite speed of light will significantly perturb the electromagnetic interaction energy between particles, giving rise to a reduced attractive force [17]. The consequences of finite light propagation, known as "retardation effects", could be modeled

[10]Static polarizability is the ability for two charge distributions—for example, atoms—to induce distortions in each other's shape, leading to an electrostatic interaction.

by the newly developed theory of quantum electrodynamics.

In 1948 Casimir and Polder extrapolated this line of thinking [18, 7]—an argument which eventually led to the parallel plates derivation. Their first paper ignored the colloidal context, however, and considered the straightforward interaction of two cases: an atom near a conducting plate, and two nearby atoms.

4.2 Atom-Plate Interactions

A neutral atom with static polarizability is placed very close to the center of one wall of a large conducting cubic cavity. Casimir begins by finding the normal modes for the electromagnetic field within the cavity, and calculates the operator $\hat{G}$ describing the atom-field interaction. Second-order perturbation theory is used to approximate the effects. As in the parallel-plates case, even the difference in energies between the near and far atom are divergent and require renormalization.

Neglecting the electromagnetic field variation within the atom gives rise to an infinite divergence in interaction energy. Instead of modeling the atomic structure rigorously, Casimir and Polder multiply the energy by a regulator $e^{-\gamma k}$. There is *also* a simple pole in the expression for electrostatic energy, which is removed by integrating very close to the pole, and avoiding it by a semicircular detour of radius z. In both cases, the functions are renormalized by taking the limit as γ and z approach zero.

The final energies were found to be

$$\delta E = -\frac{2}{\pi} \sum_n \int_0^\infty \frac{k_n u^2 du}{u^2 + k_n^2} \frac{e^{-2uR}}{2R} \times |q_{0;n}|^2 \left(1 + \frac{2}{2uR} + \frac{2}{4u^2R^2}\right), \tag{4.1}$$

where each n corresponds to the contribution from one degenerate energy level. The important thing to glean from these expressions is that the force between an atom and a conducting plane goes like R^{-3} for short distances, but shifts to R^{-4} as the distance increases. Indeed, the energy for small R is exactly the classically predicted London energy, whereas the distant interaction is modified as retardation effects become significant. Recovering the London energy in the small-scale limit suggests that the Casimir effect supersedes, rather than augments, our existing understanding of electromagnetic interactions involving neutral particles. This view is also suggested by Casimir and Polder's second case: the interaction of two atoms.

4.3 Atom-Atom Interaction

Casimir and Polder also treated the interaction between two neutral atoms, again by using perturbation theory. They took the unperturbed states to be the atomic states (independent from the field and each other) and the radiation field in empty space. The perturbation operator is then computed by adding contributions from the electrostatic interaction of the two atoms together, and their respective interactions with the electromagnetic field. The fourth-order perturbation is used to calculate the energy of interaction.

Once again, singularities in the perturbation integrals are encountered, and avoided by integrating around them in increasingly small radii. Another method that Casimir and Polder take advantage of is to shift the coordinate plane, subtracting some small value from a coordinate to "push" singularities out of the path of integration.

The subsequent nontrivial calculation reveals again that in the limit of small R, the field interaction gives rise to the same forces as the London model, which goes as R^{-6}. However, for large R, retarding effects begin to take hold, and the force begins to decrease as R^{-7}.

What is remarkable about these two derivations is that in accounting for the finite speed of light, Casimir and Polder made use of the full quantum-electrodynamic machinery in tackling a previously unconsidered problem—and discovered an unexpected result which could *also* be interpreted as an effect of the quantum vacuum.

5 Geometry Dependence

We have so far encountered three cases of the Casimir effect: two plates, a plate and an atom, and two atoms interacting with each other. In each case we have surrounded the system with a conducting cubical box to simplify the quantization conditions, but the enclosure dimensions turn out not to matter in the final approximation. Hence, we may take the limit as the box goes to the size of the universe and consider the interaction a purely local one. Moreover, we have abstracted much of the detail of the atoms away from the expressions for their energy of interaction, describing each one only by position and static polarizability. Yet the spatial dependence of the Casimir energy differs significantly between the three cases! This suggests that the Casimir force is dependent on the geometry of the system, and this is indeed the case, as has been confirmed by the plethora of theoretical papers covering various configurations of conductors in the years since the resurgence of interest in the Casimir effect in the 1970s [11].

5.1 A Spherical Shell

One of the simplest possible configurations is that of a conducting spherical shell. Given the attraction between the parallel plates and atoms discussed in the previous sections, one might expect that the Casimir force would pull a spherical shell inwards, as vacuum fluctuations outside the cavity overwhelmed those within.

Casimir suggested in 1956 that this might provide a solution to a longstanding problem in physics: the electron radius. In order to avoid an infinite charge density (and self-energy) for a point electron, some physicists suggested that the electron's charge be spread out in a spherical configuration. However, such a charge distribution would exert an outward electrostatic force which would cause the electron shell to expand. Poincaré suggested the introduction of ad-hoc forces to ensure the electron's stability. Casimir proposed that these forces (by analogy with his parallel plates derivation) could be accounted for by the zero-point energy of the configuration. Unfortunately, this turned out not to be the case.

Casimir's model proved an inspiration for Boyer, who published a rigorous derivation of the Casimir energy for spherical shells in 1968 [19]. He used the commonly known transverse and longitudinal electromagnetic modes in a spherical cavity, the same inverse-exponential cutoff frequency renormalization program used by Casimir, and the Euler-Maclaurin formula to find the zero-point energy of a double spherical cavity. In his configuration, an inner sphere with radius a was surrounded by an outer conducting "spherical universe" with radius $R \to \infty$.

Unfortunately, the full expression for the energy passes through Bessel functions on its way to a complex sum of integrals involving inverse trigonometric functions, and, being four lines long, does not lend itself well to analytic interpretation. This, sadly, is a common thread in evaluations of quantum electrodynamic effects. However, Boyer was able to produce conclusive results through numerical analysis. He found (somewhat surprisingly) that the approximation for the vacuum energy of the shell converged rapidly to

$$\langle E \rangle \approx +0.09 \frac{\hbar c}{2a}. \tag{5.1}$$

This constant was refined by Davies, Balian and Duplantier, and Leseduarte and Romeo; the currently accepted value is approximately 0.092353 [20].

Indeed, the Casimir energy is finite for this configuration, but surprisingly, its sign is positive! A spherical conducting shell, unlike any of the geometries previously discussed, tends to *expand*

due to the zero-point energy. One possible way to interpret the effect is to return to Verwey and Overbeek's retardation models [17], and to view the repulsive force on the shell as an effect of retarded dispersion forces—the interaction of instantaneous dipoles formed in the shell to negate the electric fields at the boundary. Alternatively, one could interpret the positive vacuum energy as an effect of the higher density of modes allowed by the spherical Bessel functions which describe standing waves within the cavity. Either way, the repulsive nature of the force suggests that the vacuum energy interaction cannot be viewed simply as a pressure due to constrained wavelength sizes, but is also strongly dependent on the geometry of the surface.

5.2 Corners

In our treatment of infinite plates, atoms, and spheres, we have ignored the interactions at sharp corners. In fact, the absence of corners has been an underlying assumption in our renormalization of the high frequency (ultraviolet) divergence in the zero-point energy [21]. To be exact, removing the ultraviolet divergence relies on the finite curvature of the boundary conditions: for smooth systems, contributions from both sides of the conductor cancel out.[11] Thanks to the divergence of the electromagnetic field near sharp boundaries, infinite curvature yields a divergence in the Casimir energy. The resulting force includes a positive infinite term which tends to flatten any corners in the boundary.

While the intrinsic Casimir energy of a body may be divergent, if we neglect this energy (say, by assuming a rigid body), the Casimir force *between* two bodies may yet be finite. For example, two wedges which face each other experience an attraction proportional to their dihedral angles θ [21]:

$$\langle E \rangle = -\frac{\hbar c t g^2 \theta}{4\pi^2 a} \tag{5.2}$$

However, the divergent energy near sharp corners does manifest itself physically, especially for systems of thin foils. A sheet conductor which is cut along a line, for example, experiences a strong attractive force due to the Casimir interaction which pulls the two halves back together. Even stranger, a thin metallic foil which undergoes small deformations (say, due to thermal photons) will tend to wrinkle up: ripples with wavelengths larger than 2.9 $\hbar c/T$ are amplified, and smaller ripples are flattened out. Whence [10], for nonzero temperatures, plane foils are unstable systems [21].

[11] We avoided this difficulty for the plate system by placing the boundaries far away.

6 Temperature Dependence

Our original derivation of the Casimir effect assumed the system to be at absolute zero. However, this is not the case, and we must consider thermal corrections to the vacuum energy when performing experiments on real-world systems.

6.1 Basic Thermodynamics

In addition to the vacuum energy, the walls and the field can have some non-zero temperature T. If the system is in thermal equilibrium, the field will exhibit random thermal fluctuations around its expectation value, which contribute to the energy and entropy of the system [10]. Hence we must also include the thermodynamical effect of radiation pressure within the cavity.

Consider the parallel-plates problem. If we treat the cavity walls as black-bodies, and take the free energy of the photon gas inside the cavity, the thermal part of the electromagnetic free energy of the system is [21]

$$\psi(u) = \int_u^\infty x \ln(1 - e^{-x})\, dx, \quad x = \beta\hbar\omega \tag{6.1}$$

$$F_T(a) = 2\frac{L^2}{2\pi\beta}\frac{1}{(\beta\hbar c)^2}\sum_{n=0}^{\infty}\psi(n\beta\pi\hbar c/a) \tag{6.2}$$

Taking the partial derivative of the free energy with respect to a, we obtain the force exerted on the plate due to thermal photons: the black-body radiation pressure

$$\begin{aligned} X'_T &= -\frac{\partial F_T}{\partial a} \\ &= -2\frac{L^2}{2\pi\beta a}\frac{1}{(\beta\hbar c)^2}\sum_{n=0}^{\infty} n^2(\beta\pi\hbar c/a)^2\,\psi(n\beta\pi\hbar c/a). \end{aligned} \tag{6.3}$$

As $L \to \infty$, this becomes the limit of the radiation pressure for infinite separation

$$X_T^\infty = -\frac{L^2}{\beta}\frac{1}{\beta\hbar c}\frac{\pi^2}{45}. \tag{6.4}$$

Outside the cavity, this is the radiation pressure that applies to the plates. Hence, we need to subtract this force from the force from the inside of the cavity to obtain the total thermal force

$$X_T = X'_T - X_T^\infty \tag{6.5}$$

For short distances, the $n = 0$ term vanishes and the results are dominated by a straightforward exponential decay $\psi(x) = e^{-x}$. Taking the first few terms of the sum in (6.4), we can show that the force at low temperature (or short distances) is

$$F = -L^2 \frac{\pi^2}{240} \frac{\hbar c}{L^4} - \frac{\pi^2}{45} \frac{1}{\beta} \frac{1}{(\beta \hbar c)^3} + \frac{1}{\beta} \frac{\pi}{a^3} e^{-\alpha} + \cdots \tag{6.6}$$

where $\alpha = \beta \pi \hbar c / a \ll 1$ [21]. The force due to thermal effects scales as T^4 in the first, attractive, term. For two plates roughly 1 μm apart, $\alpha \approx 24$, and the repulsive thermal forces from within the cavity are extremely small. Therefore, most of the thermal effects come from the external radiation pressure. If we neglect the internal thermal modes, the relative magnitude of the thermal force as compared to the zero-point force is

$$\gamma \approx \frac{1}{3} \left(\frac{2\pi}{\alpha} \right)^4, \tag{6.7}$$

which suggests that even at room temperature the attraction between plates is largely (γ on the order of 10^{-4}) due to quantum-mechanical effects. However, high precision experimental confirmation requires greater accuracy than these back-of-the-envelope calculations.

6.2 Numerical Modeling

Genet, Lambrecht, and Reynaud [22] suggested that thermal field fluctuations for metals most commonly used in experimental measurements would become appreciable at room temperature for distances of a few μm. They suggested that for purposes of experimental confirmation, both thermal effects and finite conductivity would need to be accounted for. In their paper, they derived corrective factors

$$\eta_F^P = \frac{F^P}{F_{Cas}}, \quad \eta_F^T = \frac{F^T}{F_{Cas}}, \tag{6.8}$$

where F_{Cas} is the regular Casimir force between two plates, and F^P and F^T are the real Casimir forces including conductivity and thermal effects, respectively.

To model conductivity, they modeled each plate as an identical mirror with a large optical thickness, such that the boundary conditions corresponded to a simple vacuum-metal transition, with reflecting behavior determined by the oscillations of electrons in the metals, with plasma frequencies drawn from the best known values for the metals commonly used in experimental measurements. While the plasma model is inaccurate for very small distances, the authors noted

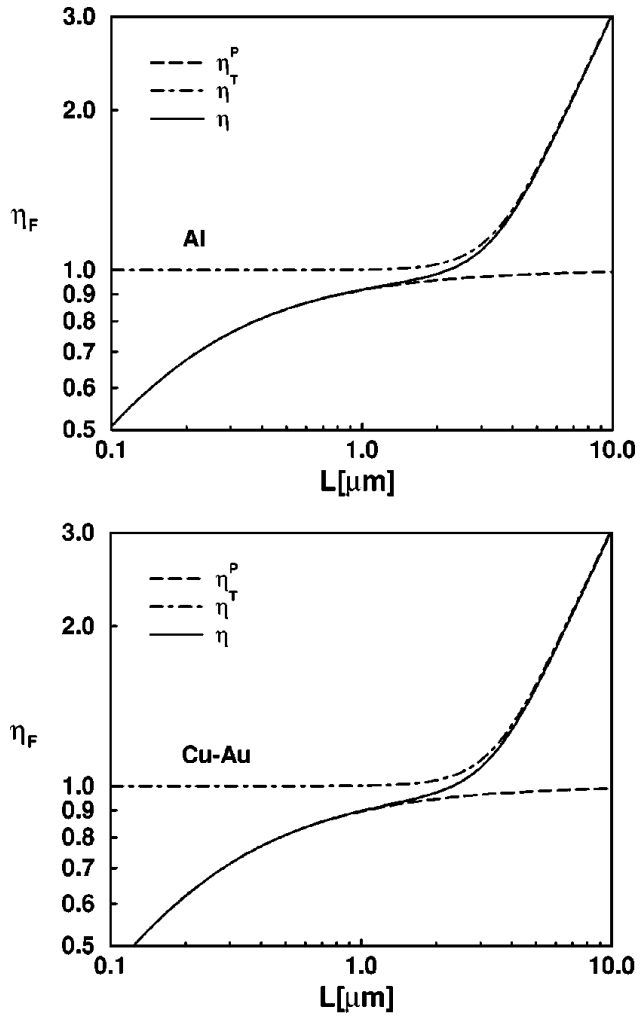

Figure 2: Correction to the Casimir force for aluminum (top) and copper/gold (bottom), as a function of distance [22]. This simulation modeled a two-mirror system at 300 Kelvin.

that the discrepancy could be corrected by making use of the real dielectric functions[12] for the metals. They also ignored any surface roughness effects, which they suggested could play a critical role.

Genet *et al* found through numerical methods that the corrective factors due to conductive and thermal interactions were largely separable from each other, with a combined corrective factor of approximately 1% [22]. However, accurate experiments require greater precision, and when the distance between plates is greater than the plasma wavelength but smaller than the thermal wavelength, the combined effects must be considered. Their work produced, for common experimental metals and configurations, plots of the force correction factors which could be used to accurately

[12]Dielectric functions give the response of the material in terms of spatial and temporal frequencies.

predict values for intermediate distances—allowing precise experimental verification.

7 Experimental Verification

Casimir remarked [7], at the conclusion of his parallel-plates derivation, that "although the effect is small, an experimental confirmation seems not unfeasible and might be of a certain interest." Since the Casimir effect is a quantum effect which may be measured for macroscopic objects, observing it would provide another confirmation of quantum electrodynamics. The first attempts to verify the effect began in the 1950s, but were unfortunately inconclusive. In this section, we will highlight a few of the experimental tests of the Casimir effect, including current topics of research.

7.1 Early Efforts

The first direct attempt at measuring the Casimir force came in 1958, when Sparnaay made measurements of the attractive force between two glass plates [23]. However, his experimental margin of error was essentially 100%. Although he made several suggestions for improved experimental technique, including the importance of clean surfaces and minimizing electrostatic attraction, experimental verification of the Casimir force proper was abandoned until 1997—despite significant theoretical developments during that time [24].

While the Casimir effect may not have been confirmed, the effects of vacuum energy were demonstrated by Sabisky and Anderson in 1972 [25]. Casimir and Polder's models for retarded dielectric interactions were extended to continuous bodies by Lifshitz, who derived an expression for the retarded interaction in terms of the dielectric functions of each media. His model simplifies, in limiting cases, to the London and Casimir-Polder interactions, which makes it an excellent way to probe the zero-point energy using extended, non-ideal boundaries. Sabisky and Anderson applied the Lifshitz equations to a oscillations of a thin film of liquid helium, demonstrating good agreement with the Lifshitz model, and by extension suggesting that the Casimir force (another consequence of nonzero vacuum energy) could be experimentally observed.

The experiment worked by depositing a very thin film of helium across the surface of an alkaline-earth fluoride crystal, which has been cleaved to yield an very flat surface—with only atom-scale variations. The film clings to the substrate through the Lifshitz interaction, and its thickness is measured by inducing acoustic standing-wave patterns between the substrate and the helium liquid-gas interface; thickness is obtained by counting wavelengths across the film. Their data (see

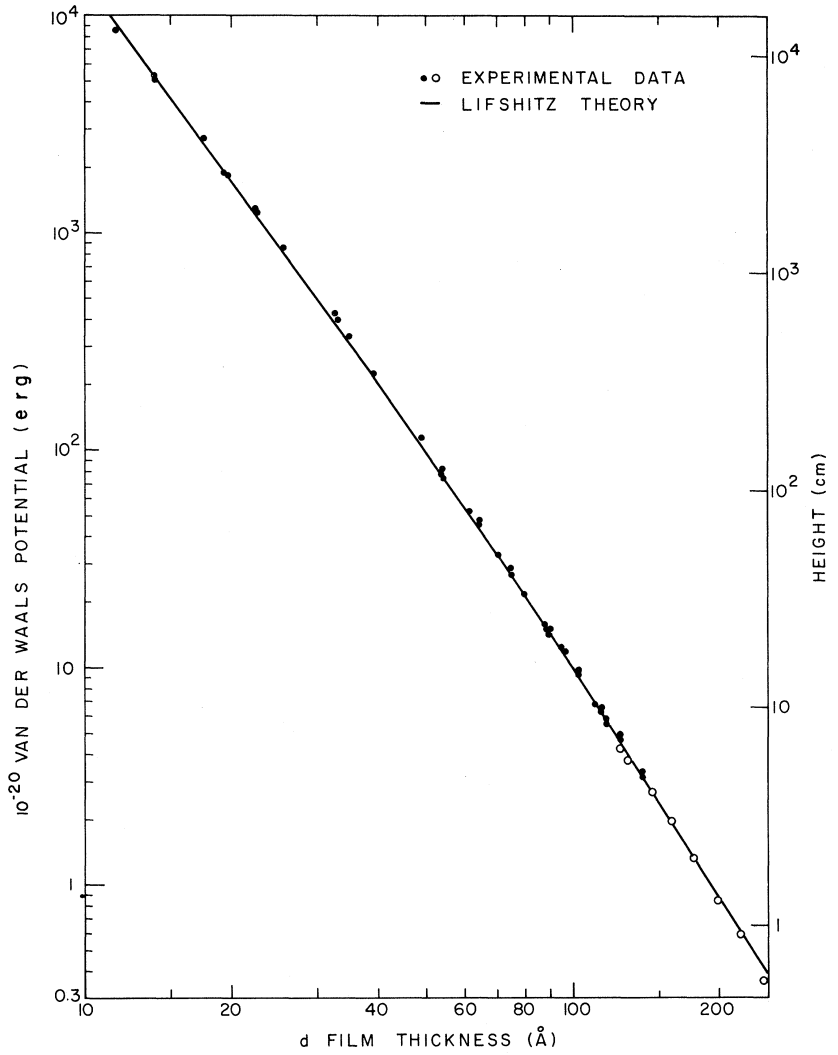

Figure 3: Sabisky and Anderson's corrected results for the van der Waals potential vs. film thickness [25]. Points represent experimental data, and the line represents the Lifshitz theory.

Figure 7.1), corrected for dispersion and phase-shifting effects, revealed excellent agreement with Lifshitz' model, hence confirming—albeit in an indirect way—the reality of vacuum forces.

7.2 Modern Experiments

In 1997, Lamoreaux demonstrated the Casimir effect using what has become the de facto standard for high-accuracy Casimir experiments: the plate-sphere configuration [24]. While the interaction between two plates is relatively straightforward to calculate, the parameter space is significantly more complex. One must control not only the distance between the plates (in nanometers), but also their relative angles in two dimensions (down to 10^-5 radians). Maintaining this degree of

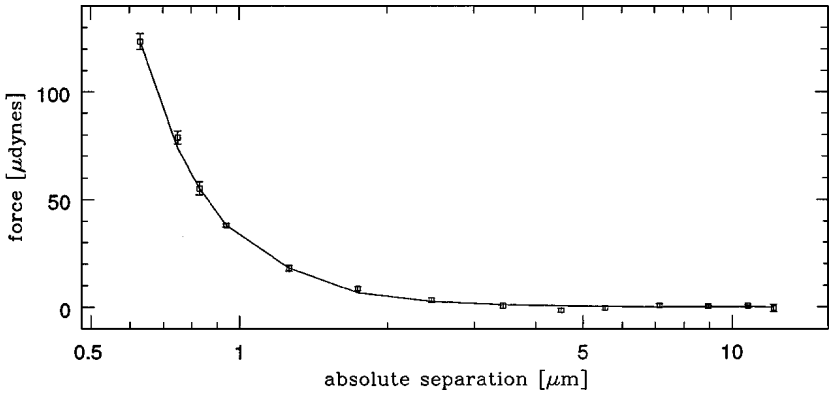

Figure 4: Lamoreaux's results for the Casimir force, plotted as a function of sphere-plate separation [24]. Data (points) show excellent agreement with the PFT model (line).

parallelism is extraordinarily difficult, and so many experiments use a plane and a sphere instead. This is possible thanks to the *Proximity Force Theorem*, or PFT, which models the sphere in terms of small plane segments with corrected areas [11]. The PFT force between a sphere and a flat surface is

$$F(a) = 2\pi R \left(\frac{1}{3} \frac{\pi^2}{240} \frac{\hbar c}{a^3} \right), \tag{7.1}$$

where R is the radius of the sphere.

The surfaces used in the experiment were actually small lenses, 2.54 centimeters in diameter, coated by evaporation with a 0.5 μm layer of copper and 0.5 μm layer of gold. The spherical electrode was attached to a micropositioning assembly to allow for fine-grained control of the sphere-plate distance. The plate, by contrast, was mounted on a small torsion rod which allowed for small angular rotation, moving the plate closer or farther from the sphere.

Measuring the distance between the plates is more complex. A stack of piezo transducers allowed the experimenters to change the distance between the plates. At each step, the voltage applied to the PZTs is adjusted to hold the pendulum at constant displacement: that voltage is proportional to the force between the plates. The distance was calibrated by measuring the change in capacitance between the plates for various separations. In addition, corrections were required for the significant (430 mV) voltage between the plates when shorted; applying a countering static voltage to the two plates throughout the experiment counteracted the effect. Because of this voltage, an electrostatic interaction known as the *contact potential* was also present in the data, varying as $1/a$.

Despite these complications, this experiment provided excellent confirmation for the Casimir force, to within five percent, for distances down to 0.6 μm. (See Figure 7.2.) This was not small

enough to resolve the corrections to the Casimir theory for thermal effects, but subsequent experiments have continued to lower the margin of error—down to less than 1% at the 95% confidence interval [26], making the plane-sphere configurations one of the most productive avenues of Casimir research in the last decade [27].

7.3 Optical Transparency

Since the experimental field has narrowed so much towards Lifshitz models of plane-sphere configurations in recent years, some researchers are pursuing another avenue of investigation: modifying the dielectric functions of the plates themselves, and measuring the change in the Casimir force at fixed distances. An excellent family of materials for this task are the Hydrogen Switchable Mirrors (HSMs)—metals such as Mg_2Ni, which switch from being reflective in air to transparent in hydrogen. Switching the HSM changes the frequencies which contribute to the Casimir energy, which manifests as a small difference in force.

Unfortunately, early experiments with HSMs have not yielded conclusive results. Iannuzzi, Lisanti, and Capazzo, in 2004, performed systematic measurements with a gold plate in proximity to an HSM-coated sphere, for distances of 70–400 nm [28]. Force measurements were made with a piezoelectric transducer directly below the gold plate, which was supported by a torsion rod. They ran oscillating electric current through the base of the plate to induce stable oscillations in the gold plate, and measured the variance of the oscillation amplitude to find the influence of the Casimir force. However, despite successfully inducing the HSM transition from reflective to transparent, both conditions yielded the same Casimir forces!

A followup paper from 2006, by de Man and Iannuzzi, examined the theoretical requirements for observing the desired shift in the Casimir energy [27]. Because the dielectric behavior of HSMs is only known for wavelengths of 0.2–2.5 μm, it is possible that the mirror surface is *not* transparent for higher (ultraviolet) ranges of the spectrum. If this were the case, it could be that the energy shift during hydrogenation could be much smaller than predicted.

Using the Lifshitz equation, de Man and Iannuzzi constructed several models for the dielectric behavior of an HSM at higher frequencies, based on the Drude-Lorentz model for metals [27]. Indeed, they found that the expected decrease in the Casimir force was significantly dependent on the imaginary-frequency behavior of the HSM's dielectric function—a factor which has not been experimentally tested. For reasonable estimates of the high-frequency dielectric behavior, de Man and Iannuzzi suggested that the difference in energy was well within the margin of error in their

earlier experiments, but could be detected with a more modern experimental apparatus. Further investigation into the behavior of the Casimir force using hydrogen switched mirrors is ongoing, and will likely prove a fruitful avenue of investigation not only for the Casimir force, but also for material science.

7.4 Repulsive Forces

The Lifshitz model predicts that some configurations may produce repulsive Casimir forces. This was recently confirmed by Capasso and Munday, who used a gold sphere and a silica plane surrounded by liquid bromobenzene [29]. The sphere, intermediate liquid, and metal plate have low, medium, and high permittivities. Thanks to the Casimir effect, larger polarizations are induced in the fluid than the low-permittivity plate. The fluid is drawn to the high-permittivity plate with a stronger force than the two plates are drawn to each other, causing a net repulsion.

Capasso and Munday's experiment made use of the same techniques discussed above: cantilevered support for the gold sphere, angular measurements using reflected light from the cantilever, and used the PFT approximation to predict the Casimir forces. They also needed to overcome some additional challenges, however, such as the drag forces due to the bromobenzine liquid. Since the drag forces are velocity-dependent, they were separated from the data by performing the experiment at multiple speeds. Their results indicated repulsive forces on the order of 10 piconewtons for separations of up to 40 nm.

7.5 Electrostatic Interactions

Measuring the Casimir effect is further complicated by the fact that electrostatic interactions also affect the plate energy. Moreover, this interaction is frequently nonlinear in experimental setups, especially if there is a uniform gradient to the work function for the cavity boundaries. The net effect is a "spurious" force between the objects comprising the boundary, which Lamoreaux identified in his research in fall of 2008 [30].

Experimenters typically work with conductive plates and spheres, and then adjust the applied voltage to their surfaces. That voltage is typically minimized for a single intermediate value before readings are taken, and then held constant. However, Lamoreaux found that the applied voltage necessary to minimize the electrostatic force in his sphere/plate experiment was actually distance-dependent!

$$V_a(d) = a \log d + b \tag{7.2}$$

In which a and b are on the order of a few mV, and d is the inter-plate distance. This potential arises from the assumption that the voltage on the surface a distance R from a plate varies as r^n for $n \ll 1$. This gives rise to a $1/d^{5/4}$ potential for the minimized force—a theoretical model matched by his experimental findings of a potential running as $1/d^{1.2-1.4}$.

It is not necessary to understand the dynamics behind this potential to correct for its effects. Lamoreaux suggested measuring the applied potential at large separations to set initial conditions, and solving the electrostatic interaction numerically. Correcting for contact potential effects is one more factor that Casimir force measurements must take into account.

8 Conclusion

We have reviewed how the Casimir energy arises from the quantization of the electromagnetic field, and derived the energy of interaction from some simple boundary conditions. Zeta-functional regularization proved an elegant, if unnerving, way to handle the infinities associated with quantum field theory. From Casimir and Polder's first suggestion of interatomic dielectric attraction to micromechanical interactions, the vacuum energy appears in a variety of contexts—and even at high temperatures and for macroscopic systems, may be experimentally confirmed. Ongoing research will begin to probe the accuracy of our models of vacuum energy, through Lifshitz's equations, for even finer effects such as variable dielectric behavior. No matter what we find, the Casimir effect will remain an unintuitive and fascinating consequence of quantum electrodynamics.

References

[1] Thomas A. Moore. *Six ideas that shaped physics—Unit R: The Laws of Physics are Frame Independent.* McGraw-Hill Higher Education, 2 edition, 2003.

An introductory text on special relativity.

[2] John S. Townsend. *A modern approach to quantum mechanics.* University Science Books, 55D Gate Five Road, Sausalito, CA 94965, 2000.

An introductory quantum mechanics text, used primarily for its derivation of the vector potential operator $\hat{\mathbf{A}}$ and the consequent quantization of the Hamiltonian.

[3] Edward M. Purcell. *Electricity and Magnetism.* McGraw-Hill, 1985.

An excellent text on classical electricity and magnetism, including relativistic digressions.

[4] Melvin Schwartz. *Principles of Electrodynamics.* McGraw-Hill, 1972.

Advanced text on electrodynamics.

[5] Hector Calderon. Personal communication, February 2009.

Discussions with my comps advisor on the Casimir's plate derivation, the philosophical implications of regularization, and more.

[6] K C Hannabuss. Commutation relations for linear fields: a coordinate-free approach. *Journal of Physics A: Mathematical and General*, 32(5):L71–L75, 1999.

A somewhat advanced theoretical article, presenting the commutation relations between the electric and magnetic fields.

[7] H.B. Casimir. On the attraction between two perfectly conducting plates. *Proc. K. Ned. Akad. Wetensch.*, 51:793–795, 1948.

Casimir's classic paper on the plane-plane energy. A much cleaner derivation than his previous investigation using retardation effects, and suitable for undergraduate reading.

[8] Jr. Frank S. Crawford. *Waves.* McGraw-Hill, 1968.

The best waves textbook ever written.

[9] Various. Euler-maclaurin formula. World Wide Web Electronic Publication, 2008.

Wikipedia article on Euler-Maclaurin summation, used for its historical discussion.

[10] Ralph Baierlein. *Thermal Physics*. Cambridge University Press, 1999.

An excellent theoretical discussion of the behavior of a photon gas from a thermodynamic perspective.

[11] M Bordag, U Mohideen, and V M Mostepanenko. New developments in the casimir effect. *Phys. Rep.*, 353(quant-ph/0106045. 1-3):1–205, 2001.

An overview of the theoretical and experimental progress in the Casimir effect since Polder and Casimir in 1948. Used mainly here for its zeta-functional regularization.

[12] Arie Kapulkin. Personal communication, February 2009.

Skype discussions concerning the zeta-functional renormalization derivation presented here, and the interpretation thereof.

[13] Jonathan Sondow and Eric W. Weisstein. Riemann zeta function, 2009.

Mathematically oriented overview on the Riemann Zeta function.

[14] James Lepowsky. Vertex operator algebras and the zeta function. *Contemporary Math*, 248, 1999.

A highly theoretical discussion of zeta-function normalization and its connections to the underlying spaces of quantum mechanical fields.

[15] S. W. Hawking. Zeta function regularization of path integrals in curved spacetime. *Communications in Mathematical Physics*, 55:133–148, 1977.

An extremely advanced survey of various applications of Zeta regularization, including the Casimir effect.

[16] Israel Klich. Photon Green's function and the Casimir energy in a medium. *Phys. Rev.*, D64:045001, 2001, hep-th/0012241.

The use of Green's functions in Casimir energy calculations. More advanced.

[17] E. J. W. Verwey and J. The. G. Overbeek. Theory of the stability of lyophobic colloids. *Elsevier, Amsterdam*, 4(541):3453, 1948.

The paper which originated the DVLO theory of colloidal solutions, extending the van der Waals forces to a more generalized model.

[18] H. B. G. Casimir and D. Polder. Influence of retardation on the london-van der waals forces. *Nature*, 158:787–788, 1948.

Casimir and Polder's original paper incorporating retardation effects into the interaction of statically polarizable atoms. Higher math.

[19] Timothy H. Boyer. Quantum electromagnetic zero-point energy of a conducting spherical shell and the casimir model for a charged particle. *Phys. Rev.*, 174(5):1764–1776, Oct 1968.

An early derivation of the energy of a spherical conducting shell, and discussion of Casimir's model for the electron's stability (building on Poincaré).

[20] K. A. Milton. *The Casimir Effect: Physical Manifestations of Zero-Point Energy*. World Scientific, 2001.

A general overview of the Casimir effect, oriented towards a wider audience.

[21] Roger Balian and Bertrand Duplantier. Geometry of the Casimir Effect. *arXiv*, 2004, quant-ph/0408124.

An excellent overview of several Casimir geometry problems, and discussions of the influence of curvature.

[22] Cyriaque Genet, Astrid Lambrecht, and Serge Reynaud. Temperature dependence of the casimir effect between metallic mirrors. *Phys. Rev. A*, 62(1):012110, Jun 2000.

A numerical evaluation of the temperature-related corrections to the Casimir force, including consideration of finite conductivity.

[23] M.J. Sparnaay. Measurements of attractive forces between flat plates. *Physica*, 24(6-10):751 – 764, 1958.

The first measurement of the Casimir effect between two plates, unfortunately inconclusive.

[24] S. K. Lamoreaux. Demonstration of the casimir force in the 0.6 to $6\mu m$ range. *Phys. Rev. Lett.*, 78(1):5–8, Jan 1997.

The first successful measurement of the Casimir force, using a ball/plate torsion assembly.

[25] E. S. Sabisky and C. H. Anderson. Verification of the lifshitz theory of the van der waals potential using liquid-helium films. *Phys. Rev. A*, 7(2):790–806, Feb 1973.

The first experimental confirmation of the Lifshitz model for dielectrics, using thin films of liquid helium. As such, it also verifies the physical reality of vacuum energy, although not the Casimir force, per se.

[26] D. E. Krause, R. S. Decca, D. López, and E. Fischbach. Experimental investigation of the casimir force beyond the proximity-force approximation. *Physical Review Letters*, 98(5):050403, 2007.

[27] S de Man and D Iannuzzi. On the use of hydrogen switchable mirrors in casimir force experiments. *New Journal of Physics*, 8(235), 2006.

A contemporary paper on the use of hydrogen-switcheable mirrors in measuring the Casimir effect, by means of their varying dielectric properties. It also provides an excellent survey of modern experimental literature, and explains the failure to provide conclusive results in the author's previous HSM experiment.

[28] Davide Iannuzzi, Mariangela Lisanti, and Federico Capasso. Effect of hydrogen-switchable mirrors on the Casimir force. *Proceedings of the National Academy of Sciences of the United States of America*, 101(12):4019–4023, 2004, http://www.pnas.org/content/101/12/4019.full.pdf+html.

An excellent modern paper on the ball/plate experiment, with a twist: modifying the dielectric properties of one of the conductors, thanks to its unusual response to hydrogen.

[29] Federico Capasso and Jeremy Munday. Measured long-range repulsive casimir-lifshitz forces. *Nature*, 457, January 2009.

Recent high-level report on experimental confirmation of the repulsive Casimir effect using thin liquid films between metals.

[30] Steve K. Lamoreaux. Electrostatic background forces due to varying contact potentials in casimir experiments. *arXiv*, 2008, 0808.0885v2 [quant-ph].

A brief theoretical discussion of contact potentials in Casimir experiments, and a procedure for correcting what prior experiments have—perhaps mistakenly—presumed to be a constant voltage.